Action Integrals for Ellipsoidal Billiards

Peter H. Richter, Andreas Wittek,

Mikhail P. Kharlamov*, and Alexej P. Kharlamov†

Institut für Theoretische Physik and Institut für Dynamische Systeme
University of Bremen, Postfach 330 440, D-28334 Bremen, Germany

* Institute of Mechanical Engineering, University of Volgograd,
GUS-400 119 Volgograd, Russia

† Physico-Technical Institute of the Ukrainian Academy of Science,
Donetsk 340006, Ukraine

E-mail: prichter@uni-bremen.de

Dedicated to Professor Siegfried Großmann

on the occasion of his 65th birthday

Z. Naturforschg. **50a** (1995) 693-710

Abstract

Integrable billiards in ellipsoidal and related shapes are discussed. The emphasis is on the computation and graphic presentation of energy surfaces in the space of action variables. Explicit results, including figures, are given for spheres, circular cylinders, planar ellipses, prolate and oblate ellipsoids.

Ich habe vorgestern die geodätische Linie für ein Ellipsoid mit drei ungleichen Achsen auf Quadraturen zurückgeführt. Es sind die einfachsten Formeln von der Welt, Abelsche Integrale, die sich in die bekannten elliptischen verwandeln, wenn man zwei Achsen gleich setzt.

Königsberg, 28. Dezember 1838

1 Introduction

The above citation[1] from a letter of Carl Gustav Jacob Jacobi to his colleague and mentor Friedrich Wilhelm Bessel, 20 years his senior, reminds us of a great period in the history of the University of Königsberg. During that same year, Bessel had succeeded to measure the first stellar parallax, for 61 Cygni, and thereby established the distance scale for neighboring stars to be on the order of 10 lightyears. Jacobi's achievement of that Christmas week may seem comparatively unpretentious, and yet, in his memorial address of 1852, one year after Jacobi's untimely death at the age of 47, L. Dirichlet praises it with the following words [1]: "Diese Jacobische Entdeckung ist die Grundlage eines der schönsten Kapitel der höheren Geometrie geworden, welches deutsche, französische und englische Mathematiker wetteifernd ausgebildet haben."[2]

Jacobi's solution of the problem of geodesic motion involves the introduction of ellipsoidal coordinates which have proven to be of utmost importance both in particle and wave mechanics. Without much exaggeration it may be said that integrability of mechanical problems is synonymous to separability which in turn means that some sort of ellipsoidal coordinates are the appropriate description [2], and elliptic or hyperelliptic integrals or functions the solution. Remember that after half a century of Legendre's single handed work on elliptic integrals, their deep mathematical nature, and elliptic functions as their inverse, were analyzed in a flash of independent activities by Abel and Jacobi, both in their mid-twenties at the time. Take that together with Jacobi's groundbreaking work in analytical mechanics where he elucidated Hamilton's partial differential equation and put it to practical use, it becomes apparent to what extent this giant influenced the field of mathematical physics.

He saw himself in the tradition of Euler, Lagrange, and Laplace, and followed their example in keeping analysis pure, i. e., free from pictures. His publications are clear and relatively easy to read even today, but they are virtually devoid of illustrations. This attitude was criticized by Klein and Sommerfeld in their work on rigid body dynamics [3], and we believe it prevented even Jacobi from seeing some of the richness that his

[1] English translation: The day before yesterday, I reduced the geodesic line for an ellipsoid with three unequal axes to quadratures. The formulas are the simplest in the world, Abelian integrals, transforming into the known elliptic ones if two axes are made equal.

[2] This discovery of Jacobi's is the foundation of one of the most beautiful chapters in advanced geometry which was shaped in the competition of German, French, and English mathematicians.

analytical results contain. The present note is an attempt to demonstrate this for the problem of billiard motion in ellipsoidal and related shapes.

The study of billiards as particularly simple examples of mechanical systems has itself a long history, and has been revived in connection with recent interest in the transition from integrable to chaotic behavior. [4], [5]. Jacobi hasn't explicitly studied billiard motion himself, but an elliptical billiard in D dimensions can always be understood as geodesic motion on a (D+1)-dimensional ellipsoid, with one axis shrinking to zero length. In that sense, Jacobi has indeed provided all solutions.

But this is only true in principle. He has not cared to present any study of the various possible types of motion, of frequencies, or of action integrals. Interest in these matters arose only much later, in connection with the development of quantum theory after 1910. Action integrals were then needed to arrive at discrete spectra via quatization of the actions in units of $\hbar$ [6]. In modern times, they are a convenient starting point, at least in principle, to discuss the breakup of invariant tori under non-integrable perturbations [7], [8], [9], [10]. Yet surprisingly few examples are known where the calculation of energy surfaces in terms of action variables has been carried out, and graphical presentations given. Our own recent work on the classical integrable cases of rigid body dynamics [11], [12] has aimed at filling this gap. The present contribution continues that effort with integrable billiards.

The paper is organized as follows. In Sec. 2 we start with the elementary cases of spheres and cylinders. In order to give an introduction to the specific new features in ellipsoidal shapes, we first treat the two-dimensional case of billiard in an ellipse, in Sec. 3; it is well known that there exists a separatrix between two different types of motion. For the cases treated in Secs. 2 and 3 we also present all information about frequencies and winding ratios. The rest of the paper is devoted to ellipsoidal billiards in three dimensions, with explicit results on energy surfaces for ellipsoids with rotational symmetry: prolate ellipsoids in Sec. 4, and oblate ellipsoids in Sec. 5. We do not treat these billiards as four-dimensional geodesic flow squeezed in one dimension, but rather directly evaluate the Hamiltonian of three-dimensional free motion with elastic reflection, using appropriate coordinates. In the last Sec. 6 we present the analytic basis for a similar study of the general case, but the numerical and graphical evaluation is left for the future.

The analytic complexity of a billiard inside a D-dimensional ellipsoid is the same as that of geodesic flow on the surface of a D-dimensional ellipsoid. As Jacobi remarked in his note to Bessel, the general case of geodesic motion on the surface of three-dimensional ellipsoids involves Abelian, or hyperelliptic, integrals. Taking into account the motion inside such ellipsoids does not increase this complexity. In ellipsoids with rotational symmetry, the Abelian integrals reduce to ordinary elliptic integrals for which there exists readily available numerical software. This has determined the choice of problems treated in this note.

2 Spheres and cylinders

Consider first a freely moving point of unit mass inside a sphere of unit radius, elastically reflected upon encounter with the surface. It is well known that this situation is separable in spherical coordinates r, ϑ, φ, in which the Hamiltonian reads

$$H \;=\; \frac{1}{2}\, {p_r}^2 \;+\; \frac{1}{2r^2}\, {p_\vartheta}^2 \;+\; \frac{1}{2r^2 \sin^2\vartheta}\, {p_\varphi}^2 \;, \tag{1}$$

together with the reflection condition

$$(p_r, p_\vartheta, p_\varphi) \;\rightarrow\; (-p_r, p_\vartheta, p_\varphi) \;. \tag{2}$$

There are three obvious constants of motion: energy H, the total angular momentum squared, ${p_\vartheta}^2 + {p_\varphi}^2/\sin^2\vartheta$, and the z-component of the angular momentum, p_φ. Their respective constant values will be called $E, L^2 =: 2El^2$, and $P_\varphi =: \sqrt{2E}\, l_\varphi$. The admissable ranges are $0 \le l^2 \le 1$, $-l \le l_\varphi \le l$; energy E is a scaling parameter and, without loss of generality, may be put equal to $1/2$. Except for critical cases to be discussed separately, every allowed triple (E, l^2, l_φ) defines a 3-torus[3] in phase space. Three natural fundamental cycles around these tori are

$$C_\varphi :\; dr = d\vartheta = 0 \;, \qquad C_\vartheta :\; dr = d\varphi = 0 \;, \qquad C_r :\; d\varphi = d\vartheta = 0 \;; \tag{3}$$

The corresponding actions are easily determined:

$$\begin{aligned}
I_1 \;\equiv\; \frac{I_\varphi}{\sqrt{2E}} \;&=\; \frac{1}{2\pi} \oint_{C_\varphi} \frac{p_\varphi}{\sqrt{2E}}\, d\varphi = l_\varphi \\
I_2 \;\equiv\; \frac{I_\vartheta}{\sqrt{2E}} \;&=\; \frac{1}{2\pi} \oint_{C_\vartheta} \frac{p_\vartheta}{\sqrt{2E}}\, d\vartheta = \frac{1}{2\pi} \oint \sqrt{l^2 - {l_\varphi}^2/\sin^2\vartheta}\; d\vartheta \;=\; l - |l_\varphi| \\
I_3 \;\equiv\; \frac{I_r}{\sqrt{2E}} \;&=\; \frac{1}{2\pi} \oint_{C_r} \frac{p_r}{\sqrt{2E}}\, dr \;= \frac{1}{2\pi} \oint \sqrt{1 - l^2/r^2}\; dr \\
&\qquad\qquad = \frac{1}{\pi} \left(\sin\phi - \phi\, |\cos\phi|\right) \quad \text{where} \quad \cos\phi = l \;.
\end{aligned} \tag{4}$$

The angle ϕ $(0 \le \phi \le \pi/2)$ has a simple interpretation as being the angle between a trajectory and the tangent plane to the sphere at the point of its last reflection; this is obviously a constant of the motion.

With these formulas we may plot the energy surface E =const in action space, as shown in Fig. 1. It has the shape of half a tent, symmetric with respect to the plane $I_1 = 0$, and piecewise linear ($|I_1| + I_2 = l$) in cross sections I_3 =const. The full five dimensional energy surface should be visualized as a standard 3-torus of angle variables being attached to each

[3]The discontinuities in momenta associated with elastic reflection present can be dealt with in such a way as not to destroy the picture provided by the Liouville-Arnol'd theorem.

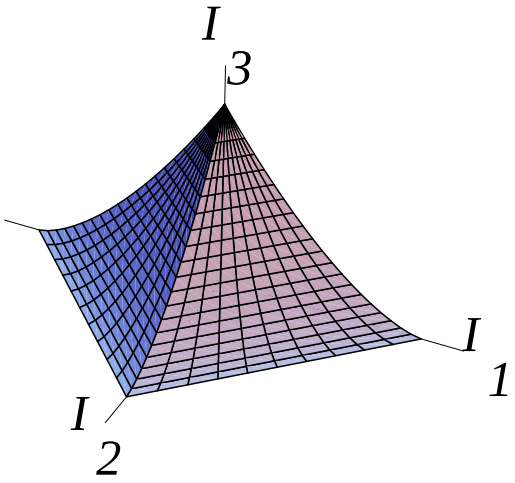

Figure 1: Energy surface of a spherical billiard. The actions are plotted in units of $\sqrt{2E}$. I_1 is the z-component of the angular momentum, I_2 the action of the ϑ-motion, and I_3 the action of radial motion. I_3 depends only on the total angular momentum $|I_1| + I_2$. Lines I_3 =const are drawn for equidistant values of the total angular momentum.

point of this 2D-surface. When one of the three actions vanishes, the 3-torus degenerates to a 2-torus or else becomes foliated by 2-tori. Thus $I_r = 0$ characterizes geodesic motion on the surface of the sphere ($r = 1$); for $I_\vartheta = 0$ the billiard takes place in the equatorial plane $\vartheta = \pi/2$. Both situations are critical cases, corresponding to 2-tori in phase space. On the other hand, the condition $I_\varphi = 0$ holds for planar billiards where φ =const, each constant between 0 and 2π labelling a different 2-torus. In the four corner points of the tent, the tori degenerate even further. The top $(I_1, I_2, I_3) = (0, 0, 1/\pi)$ corresponds to linear periodic motion through the sphere's center, with zero angular momentum, and arbitrary direction. The points $(I_1, I_2, I_3) = (\pm 1, 0, 0)$ represent circular motion along the equator, in the two possible directions; these are two 1-tori in phase space. Finally, the point $(0, 1, 0)$ characterizes circular motion in planes φ =const.

The period of the r-motion, from minimum to maximum and back to minimum, is $T_r = 2\pi/\omega_r$,

$$T_r \;=\; 2\pi \left.\frac{\partial I_r}{\partial E}\right|_{I_1,I_2} \;=\; 2\,\frac{\sin\phi}{\sqrt{2E}}\;. \tag{5}$$

The period T_ϑ of the ϑ-motion is most easily obtained from (5) and the winding ratio

$$W_{\vartheta,r} \;:=\; \frac{T_r}{T_\vartheta} \;=\; \frac{\omega_\vartheta}{\omega_r} \;=\; -\left.\frac{\partial I_r}{\partial I_\vartheta}\right|_{E,I_\varphi} \;=\; \frac{\phi}{\pi}\;. \tag{6}$$

The period T_φ of the φ-motion is the same, as can be inferred from the winding ratio

$$W_{\varphi,\vartheta} \;:=\; \frac{\omega_\varphi}{\omega_\vartheta} \;=\; -\left.\frac{\partial I_\vartheta}{\partial I_\varphi}\right|_{E,I_r} \;=\; \mathrm{sgn}(l_\varphi) \;=\; \pm 1 \;. \tag{7}$$

This degeneracy is related to the fact that any given motion takes place in a plane perpendicular to the fixed angular momentum vector. The normal to this plane has an angle $\arccos(l_\varphi/l)$ with respect to the z-axis. The identity of the two frequencies ω_φ and ω_ϑ reflects the absence of precession. For the 3-tori at given actions this means they are foliated by 2-tori.

For comparison, consider a cylindrical billiard, of radius $r = 1$ and height h. The Hamiltonian in cylindrical coordinates reads

$$H \;=\; \frac{1}{2}\,{p_r}^2 \;+\; \frac{1}{2r^2}\,{p_\varphi}^2 \;+\; \frac{1}{2}\,{p_z}^2 \;, \tag{8}$$

and again we assume elastic reflection at the surface. The constants of motion are the total energy $H = E$, angular momentum $p_\varphi = P_\varphi =: \sqrt{2E}\,l_\varphi$, and the energy of the z-motion, ${p_z}^2/2 = E_z =: Ee_z$. The natural choice of actions at given values (E, l_φ, e_z) leads to

$$\begin{aligned}
I_1 \;&\equiv \frac{I_\varphi}{\sqrt{2E}} = l_\varphi \\
I_2 \;&\equiv \frac{I_z}{\sqrt{2E}} = \frac{h}{\pi}\,\sqrt{e_z} \\
I_3 \;&\equiv \frac{I_r}{\sqrt{2E}} = \frac{1}{2\pi}\,\oint \sqrt{1 - e_z - {l_\varphi}^2/r^2}\;dr \\
&\qquad = \frac{1}{\pi}\,\sqrt{1-e_z}\;\left(\sin\phi - \phi\,|\cos\phi|\right) \qquad \text{with} \quad \cos\phi = |l_\varphi|/\sqrt{1-e_z}\;.
\end{aligned} \tag{9}$$

The angle ϕ is again the angle between the tangent plane to the cylinder's lateral surface and a trajectory after reflection. Taking the differential of the last equation, we find the following expressions for frequencies, or periods:

$$\omega_r \;=\; \left.\frac{\partial E}{\partial I_3}\right|_{I_1,I_2} \;=\; \pi\,\sqrt{2E}\;\frac{\sqrt{1-e_z}}{\sin\phi} \tag{10}$$

$$\omega_z \;=\; \left.\frac{\partial E}{\partial I_2}\right|_{I_1,I_3} \;=\; \frac{\pi}{h}\,\sqrt{2E\,e_z} \tag{11}$$

$$W_{\varphi,r} \;=\; \frac{\omega_\varphi}{\omega_r} \;=\; -\left.\frac{\partial I_3}{\partial I_1}\right|_{E,I_2} \;=\; \pm\frac{\phi}{\pi} \tag{12}$$

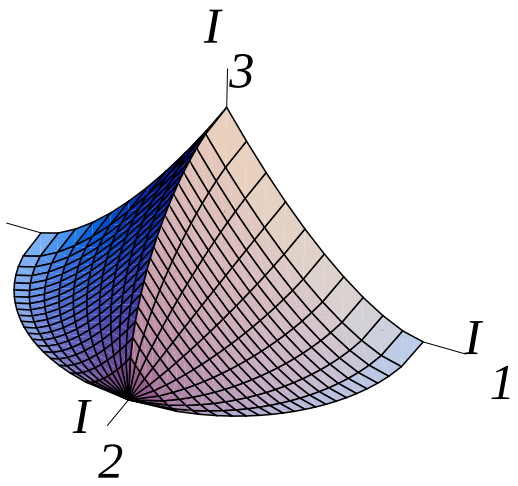

Figure 2: Energy surface of a cylindrical billiard, $h = r = 1$. I_1 is the z-component of the angular momentum, I_2 is the action of motion along the z-direction, I_3 is the action of radial motion.

The energy surface in action space is shown in Fig. 2. On the plane $I_z = 0$ it coincides with the $I_\vartheta = 0$ limit of the spherical billiard; both cases represent a planar circular billiard of radius 1. For $I_r = 0$ the motion takes place on the cylinder's lateral surface, and for $I_\varphi = 0$ on a rectangle $\varphi =$const. The corresponding lines on the energy surface are half or quarter ellipses, respectively,

$$I_\varphi{}^2 + \frac{\pi^2}{h^2}\, I_z{}^2 \;=\; 2E \qquad (I_r = 0)\ , \tag{13}$$

$$\pi^2 I_r{}^2 + \frac{\pi^2}{h^2}\, I_z{}^2 \;=\; 2E \qquad (I_\varphi = 0)\ . \tag{14}$$

3 The planar elliptic billiard

Consider the following elliptic boundary in the (x, y)-plane,

$$x^2 \; + \; \frac{y^2}{1-a^2} \; = \; 1 \qquad (0 \le a < 1) \; . \tag{15}$$

With a varying from 0 to 1, we have a family of boundaries connecting circles to thin slabs. The major half axes of all these ellipses are normalized to 1. Their foci are at $(x, y) = (\pm a, 0)$.

A natural system of orthogonal coordinates (ξ, η) is given by the sets of confocal ellipses ξ =const and hyperbolas η =const [13]:

$$(x, y) \; = \; \left(\frac{1}{a}\, \xi\eta, \; \pm \frac{1}{a} \sqrt{(\xi^2 - a^2)(a^2 - \eta^2)} \right) \tag{16}$$

where the coordinate ranges are

$$a \le \xi \le 1 \; , \qquad -a \le \eta \le a \; . \tag{17}$$

Two sheets of this coordinate set are needed to cover the $y > 0$ and $y < 0$ halves of the billiard.

The Hamiltonian of free motion inside the billiard, in terms of (ξ, η)-coordinates and corresponding momenta (p_ξ, p_η), reads

$$H \; = \; \frac{1}{2} \, \frac{1}{\xi^2 - \eta^2} \, \left((\xi^2 - a^2) {p_\xi}^2 \; + \; (a^2 - \eta^2) {p_\eta}^2 \right) \; . \tag{18}$$

Two types of reflection must be considered. One is the physical reflection at the boundary $\xi = 1$,

$$(\xi, \eta, p_\xi, p_\eta) \to (\xi, \eta, -p_\xi, p_\eta) \tag{19}$$

without change of coordinate sheet. The other is a formal reflection whenever the sheet boundaries $\xi = a$ or $\eta = \pm a$ are reached during the motion. At $\xi = a$, the rule (19) applies together with a change of sheet. Similarly at $\eta = \pm a$, there is a change of sign in p_η, together with a change of coordinate sheet. (The formal reflection might be turned into a physical one by considering a billiard in a half-ellipse.)

The elliptical billiard is integrable as the two coordinates ξ and η can be separated. Multiplying Eq. (18) by $\xi^2 - \eta^2$, we find a separation constant K:

$$2E\xi^2 - (\xi^2 - a^2) {p_\xi}^2 \; = \; K \; =: 2E\, \kappa^2 \tag{20}$$

$$2E\eta^2 + (a^2 - \eta^2) {p_\eta}^2 \; = \; K \; =: 2E\, \kappa^2 \; . \tag{21}$$

For the scaled constant of motion κ^2, it is easy to see that the allowed range of values is $0 \le \kappa^2 \le 1$. The case $\kappa = 0$ corresponds to a motion where $(\eta, p_\eta) = (0, 0)$, i. e., oscillation along the y-axis. The other extreme case, $\kappa = 1$, holds for $(\xi, p_\xi) = (1, 0)$

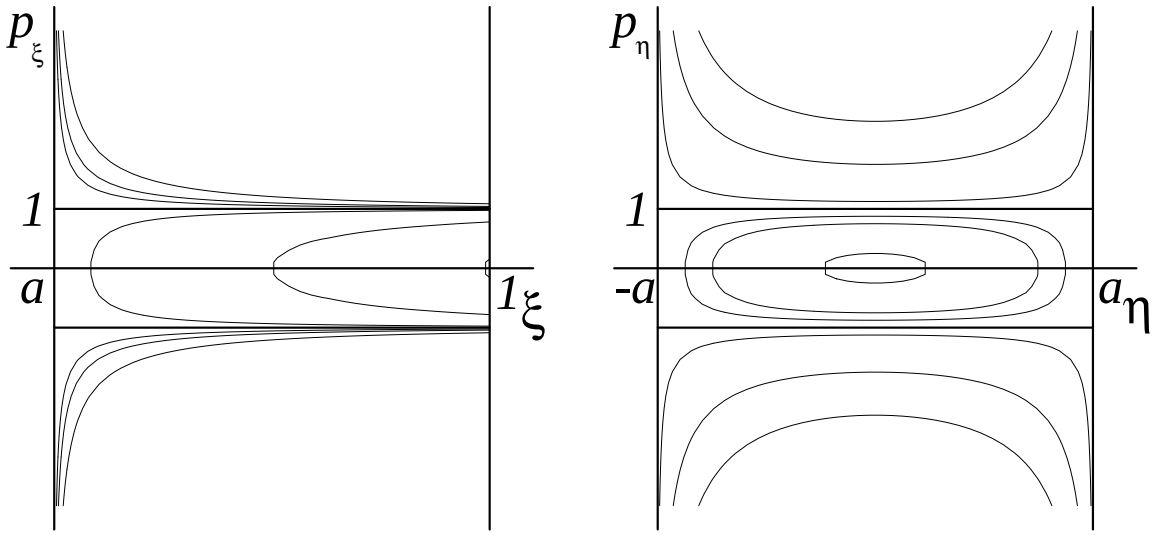

Figure 3: Phase portraits of the planar elliptic billiard; $a = 0.4$, κ-values 0.1, 0.3, 0.35, 0.4, 0.45, 0.7, 0.99. Left: intersection of invariant tori with the (ξ, p_ξ)-plane; right: intersection of invariant tori with the (η, p_η)-plane. The outermost curves of the left picture correspond to the center at right; the outermost curves of the right picture correspond to the point $(\xi, p_\xi) \approx (1, 0)$. Note that if this set of pictures is meant to describe motion in the upper half plane, $y > 0$, another such set is needed for the lower half plane, $y < 0$.

which characterizes sliding motion along the billiard's boundary. To get an intuition about the meaning of κ consider the limit $a \to 0$ where the ellipse degenerates into a circle. The relation of elliptic and ordinary polar coordinates is then $(\xi, \eta) \to (r, a\cos\varphi)$ which implies $(p_\xi, p_\eta) \to (p_r, -p_\varphi/a\sin\varphi)$. Therefore $\kappa^2 \to {l_\varphi}^2$; not surprisingly, κ^2 generalizes the angular momentum squared.

Let us discuss the invariant tori defined by given values of E (which can be assumed 1, as always in billiards without potential) and κ. Their intersections with the (ξ, p_ξ)- and (η, p_η)-planes are obtained by solving Eqs. (20) and (21) for p_ξ and p_η:

$$ {p_\xi}^2 \;=\; 2E\,\frac{\xi^2-\kappa^2}{\xi^2-a^2}\;, \qquad {p_\eta}^2 \;=\; 2E\,\frac{\kappa^2-\eta^2}{a^2-\eta^2}\;. \tag{22} $$

Fig. 3 shows that there are two types of tori, with a dividing separatrix. For $\kappa^2 > a^2$, the ξ-values are restricted by $\kappa \le \xi \le 1$, whereas η can assume all values. We call these tori type I; they resemble those in a circular billiard, ξ corresponding to the radial, η to the angular coordinate. In configuration space, the ellipse $\xi = \kappa$ plays the role of an inner envelope to the motion, where p_ξ becomes zero and changes sign. For $\kappa^2 < a^2$, on the other hand, there are no restrictions on ξ but on η: $-\kappa \le \eta \le \kappa$. We call these tori type II; they resemble those in rectangular billiards, ξ playing the role of the y-coordinate, and

η of x. The hyperbolas $\eta = \pm\kappa$ act as the vertical reflecting boundaries. The separatrix motion ($\kappa^2 = a^2$) is the only one that reaches the foci. It is asymptotic to the unstable oscillation along the x-axis.

We can now turn to the computation of the actions. The two cases of type I and type II motion must be distinguished, and care must be taken to identify closed paths around the tori, given the two coordinate sheets. Let us begin with type I orbits, $\kappa^2 > a^2$. The corresponding tori have a radial ξ- and an angular η-coordinate. The η-coordinate, using both sheets, encircles the foci in opposite senses which we shall distinguish by a $\pm$ sign. Taking the action along one full loop, we are led to a complete elliptic integral,

$$I_1 \equiv \frac{I_\eta}{\sqrt{2E}} = \frac{1}{2\pi}\oint \frac{p_\eta}{\sqrt{2E}}\, d\eta = \pm\frac{2}{\pi}\int_0^a \sqrt{\frac{\kappa^2-\eta^2}{a^2-\eta^2}}\, d\eta = \pm\frac{2\kappa}{\pi}\,\mathcal{E}(\frac{a}{\kappa})\ . \tag{23}$$

The ξ-action requires a ξ-integration from minimum (κ) to maximum (1) and back to minimum:

$$I_2 \equiv \frac{I_\xi}{\sqrt{2E}} = \frac{1}{2\pi}\oint \frac{p_\xi}{\sqrt{2E}}\, d\xi = \frac{1}{\pi}\int_\kappa^1 \sqrt{\frac{\xi^2-\kappa^2}{\xi^2-a^2}}\, d\xi\ . \tag{24}$$

This is an incomplete elliptic integral which may be expressed in terms of canonical forms [14], [15], [16]:

$$I_2 = \frac{1}{\pi}\left(\sin\phi - \kappa\,\mathcal{E}(\phi,\frac{a}{\kappa})\right)\ , \qquad \text{with} \quad \sin^2\phi = \frac{1-\kappa^2}{1-a^2}\ . \tag{25}$$

We use the notation $\mathcal{E}(\phi,k)$ for incomplete, and $\mathcal{E}(k)$ for complete, elliptic integrals of the second kind, with amplitude ϕ and modulus k.

Together, the results (23) and (25) define the two components of the type I branch of the energy surface. In the limit $a \to 0$, the planar circular billiard should be recovered, i. e., the $I_2 = 0$ result of the spherical and cylindrical billiards. This is indeed the case, as $\xi \to r$, $p_\xi \to p_r$, $\kappa^2 \to p_\varphi^2/2E$, $\cos\phi = p_\varphi/\sqrt{2E}$, and $\mathcal{E}(\phi,0) = \phi$, $\mathcal{E}(0) = \pi/2$, so that

$$I_\xi \to \frac{\sqrt{2E}}{\pi}\,(\sin\phi - \phi|\cos\phi|) = I_r \qquad \text{and} \qquad I_\eta \to p_\varphi = I_\varphi\ . \tag{26}$$

The limits $\kappa^2 \to 1$ and $\kappa^2 \to a^2+$ can also be treated explicitly. Evaluating the integral (24) for κ near 1, and using $\partial\mathcal{E}(k)/\partial k = (\mathcal{E}(k) - \mathcal{K}(k))/k$ in (23), $\mathcal{K}(k) = \mathcal{F}(\frac{\pi}{2},k)$ being elliptic integrals of the first kind, we get

$$\begin{aligned} I_1 &\approx \pm\frac{1}{\pi}\,(2\mathcal{E}(a) - (1-\kappa^2)\mathcal{K}(a)) \\ I_2 &\approx \frac{1}{3\pi}\,\frac{(1-\kappa^2)^{3/2}}{\sqrt{1-a^2}} \end{aligned} \qquad (\kappa \to 1)\ . \tag{27}$$

This describes the "whispering gallery" behavior of the elliptical billiard. The action values at the separatrix $\kappa^2 = a^2$, coming down from $\kappa^2 > a^2$, are determined by elementary integration:

$$\begin{aligned} I_1 &= \pm\frac{2a}{\pi} \\ I_2 &= \frac{1-a}{\pi} \end{aligned} \qquad (\kappa^2 \;=\; a^2+) \; . \tag{28}$$

Let us now determine the actions of type II motion, $\kappa^2 < a^2$. The η-motion is now also oscillatory, but it suffices to stay between $-\kappa$ and κ on a single sheet. I_η is therefore continuous at the separatrix. We obtain

$$I_1 \;\equiv\; \frac{I_\eta}{\sqrt{2E}} \;=\; \frac{2}{\pi}\int\limits_0^\kappa \sqrt{\frac{\kappa^2-\eta^2}{a^2-\eta^2}}\; d\eta \;=\; \frac{2}{\pi}\left(a\,\mathcal{E}(\frac{\kappa}{a}) - \frac{a^2-\kappa^2}{a}\,\mathcal{K}(\frac{\kappa}{a})\right) \; . \tag{29}$$

There is only one sign because of the oscillatory character.

In ξ-direction, to get a complete path around an invariant torus, both coordinate sheets must be traversed back and forth. At the separatrix, this makes for a jump by a factor of 2 in I_ξ. We get

$$\begin{aligned} I_2 \;\equiv\; \frac{I_\xi}{\sqrt{2E}} \;&=\; \frac{2}{\pi}\int\limits_a^1 \sqrt{\frac{\xi^2-\kappa^2}{\xi^2-a^2}}\; d\xi \qquad (30) \\ &=\; \frac{2}{\pi}\left(\sin\psi + \frac{a^2-\kappa^2}{a}\,\mathcal{F}(\psi,\frac{\kappa}{a}) - a\,\mathcal{E}(\psi,\frac{\kappa}{a})\right) \; , \quad \text{with} \quad \sin^2\psi = \frac{1-a^2}{1-\kappa^2} \; . \end{aligned}$$

The limit $\kappa \to 0$ can be obtained by elementary integration. We find

$$\begin{aligned} I_1 &\approx \frac{\kappa^2}{2a} \\ I_2 &\approx \frac{2}{\pi}\left(\sqrt{1-a^2} - \frac{\kappa^2}{2a}\arccos a\right) \end{aligned} \qquad (\kappa \to 0) \; . \tag{31}$$

This makes for a linear relation between the two actions, in this limit.

Fig. 4 summarizes the results (23), (25), (29), and (30) for a number of different a. For given a, the energy surface consists of three continuous pieces, each characterized by its particular type of η-motion: clockwise rotation outside the foci (high I_η, low I_ξ), oscillation between the foci (low I_η, high I_ξ), and anticlockwise rotation outside the foci (negative I_η).

The energy surface contains all information about frequencies and winding ratios. The easiest quantity to be derived from the above results is the winding ratio

$$W_{\eta,\xi} \;\equiv\; \frac{\omega_\eta}{\omega_\xi} \;=\; -\left.\frac{\partial I_\xi}{\partial I_\eta}\right|_E \;=\; -\frac{\partial I_\xi/\partial K|_E}{\partial I_\eta/\partial K|_E} \; . \tag{32}$$

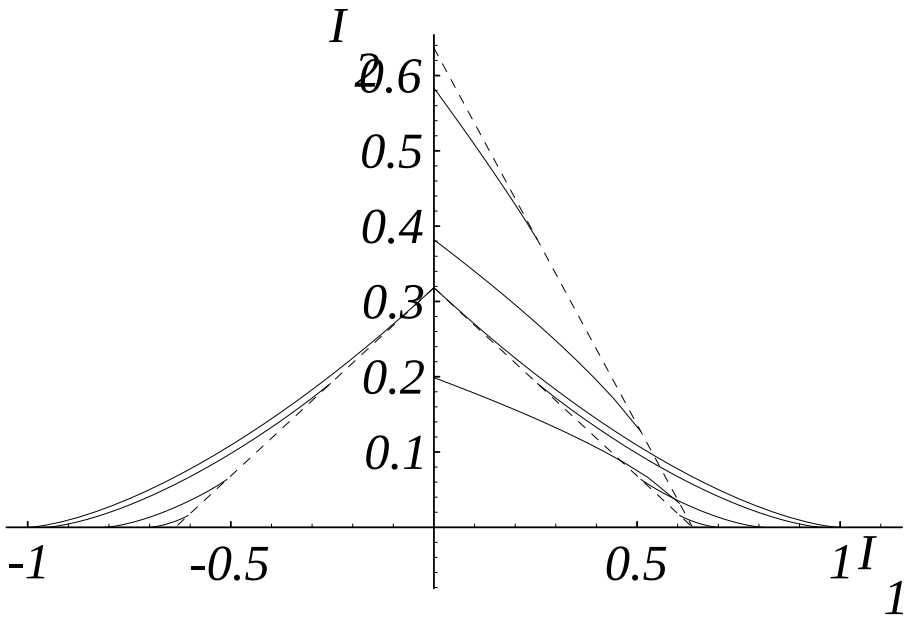

Figure 4: Energy "surfaces" of elliptical billiards. The action I_1 of (angular) η-motion is plotted versus I_2, the action of (radial) ξ-motion, for different values of a: a =0, 0.4, 0.8, 0.95. Note the different scales for I_1 and I_2. Except for $a = 0$, each energy surface consists of three pieces, two with high $|I_1|$ representing rotation of η, one with low I_1 and high I_2, representing motion between the foci. The dotted lines connect the loci of separatrix motion, cf. Eq. (28) for the lower branch.

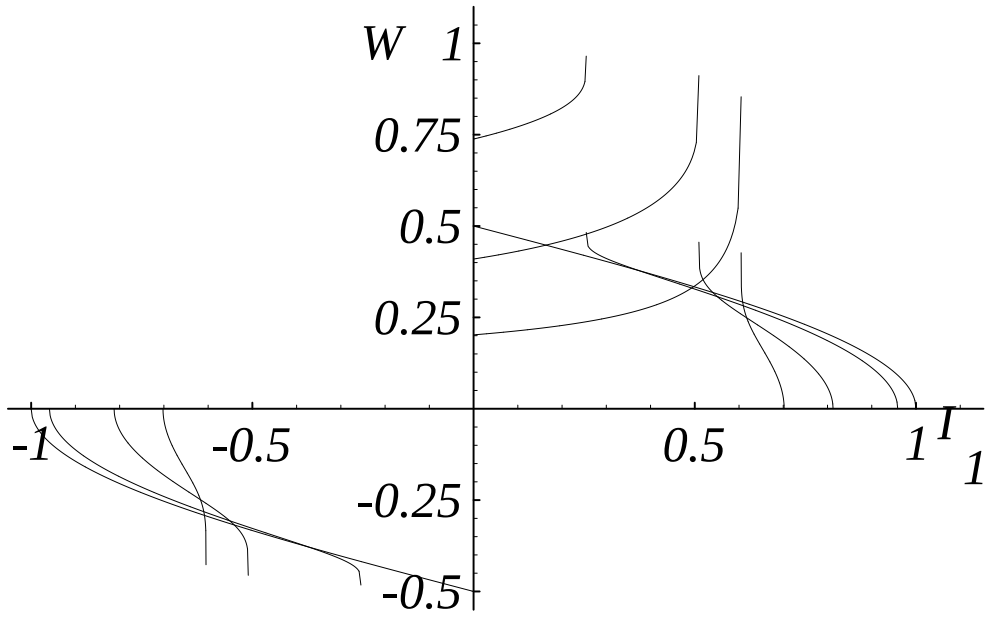

Figure 5: Winding ratio $W_{\eta,\xi}$ for elliptical billiards, plotted against I_1. The values of a are the same as in Fig. 4. Separatrices show up with typical logarithmic divergence.

Taking the derivatives with respect to the separation constant K in the integrals defining the actions, we find

$$W_{\eta,\xi} \;=\; \begin{cases} \pm\dfrac{1}{2}\,\dfrac{\mathcal{F}(\phi, a/\kappa)}{\mathcal{K}(a/\kappa)} & (a < \kappa \leq 1) \\[2ex] \dfrac{\mathcal{F}(\psi, \kappa/a)}{\mathcal{K}(\kappa/a)} & (0 \leq \kappa < a) \end{cases} \tag{33}$$

The asymptotic behavior as $\kappa \to 1$ and $\kappa \to 0$ is

$$W_{\eta,\xi} \;\to\; \begin{cases} \pm\dfrac{1}{2\mathcal{K}(a)}\,\sqrt{\dfrac{1-\kappa^2}{1-a^2}} & (\kappa \to 1) \\[2ex] \dfrac{2}{\pi}\,\arccos a & (\kappa \to 0) \end{cases} \tag{34}$$

Fig. 5 shows how the winding ratio varies as a function of the action I_η, for the same values of a as in Fig. 4.

It is a little more difficult to obtain the individual frequencies ω_ξ and ω_η. Of course, it suffices to compute ω_ξ because ω_η can then be obtained with the help of (33). Considering I_ξ and I_η as functions of E and K, we use

$$\frac{1}{\omega_\xi} \;=\; \left.\frac{\partial I_\xi}{\partial E}\right|_{I_\eta} \;=\; \left.\frac{\partial I_\xi}{\partial E}\right|_{K} \;+\; \left.\frac{\partial I_\xi}{\partial K}\right|_{E} \left.\frac{\partial K}{\partial E}\right|_{I_\eta} \;=$$

$$= \left.\frac{\partial I_\xi}{\partial E}\right|_K - \left.\frac{\partial I_\xi}{\partial I_\eta}\right|_E \left.\frac{\partial I_\eta}{\partial E}\right|_K = \left.\frac{\partial I_\xi}{\partial E}\right|_K + W_{\eta,\xi} \left.\frac{\partial I_\eta}{\partial E}\right|_K \tag{35}$$

to determine ω_ξ. So all we need besides the winding ratio $W_{\eta,\xi}$ are the two derivatives of the actions with respect to E, at constant K. This is best done directly under the defining integrals. For $a < \kappa < 1$, we find

$$\begin{aligned} \left.\frac{\partial I_\xi}{\partial E}\right|_K &= \frac{1}{\pi\sqrt{2E}} \left(\sin\phi + \kappa\, \mathcal{F}(\phi, \frac{a}{\kappa}) - \kappa\, \mathcal{E}(\phi, \frac{a}{\kappa})\right) \\ \left.\frac{\partial I_\eta}{\partial E}\right|_K &= \mp\frac{2\kappa}{\pi\sqrt{2E}} \left(\mathcal{K}(\frac{a}{\kappa}) - \mathcal{E}(\frac{a}{\kappa})\right) \end{aligned} \tag{36}$$

which may be combined with (35) and (33) to give the ξ-period

$$T_\xi = \frac{2\pi}{\omega_\xi} = \frac{2}{\sqrt{2E}} \left(\sin\phi - \kappa\, \mathcal{Z}(\phi, \frac{a}{\kappa})\right) \tag{37}$$

where

$$\mathcal{Z}(\phi, k) = \mathcal{E}(\phi, k) - \mathcal{E}(k)\, \mathcal{F}(\phi, k)/\mathcal{K}(k) \tag{38}$$

is Jacobi's Zeta-function. Note that $\mathcal{Z}(\phi, 0) = 0$.

Very similar relations can be derived for the parameter range $0 \le \kappa < a$. Using

$$\begin{aligned} \left.\frac{\partial I_\xi}{\partial E}\right|_K &= \frac{2}{\pi\sqrt{2E}} \left(\sin\psi + a\, \mathcal{F}(\psi, \frac{\kappa}{a}) - a\, \mathcal{E}(\psi, \frac{\kappa}{a})\right) \\ \left.\frac{\partial I_\eta}{\partial E}\right|_K &= -\frac{2a}{\pi\sqrt{2E}} \left(\mathcal{K}(\frac{\kappa}{a}) - \mathcal{E}(\frac{\kappa}{a})\right) \end{aligned} \tag{39}$$

we obtain the ξ-period from

$$T_\xi = \frac{2\pi}{\omega_\xi} = \frac{4}{\sqrt{2E}} \left(\sin\psi - a\, \mathcal{Z}(\psi, \frac{\kappa}{a})\right) . \tag{40}$$

Fig. 6 presents the results as functions of I_η, for the same a-values as in Fig. 4.

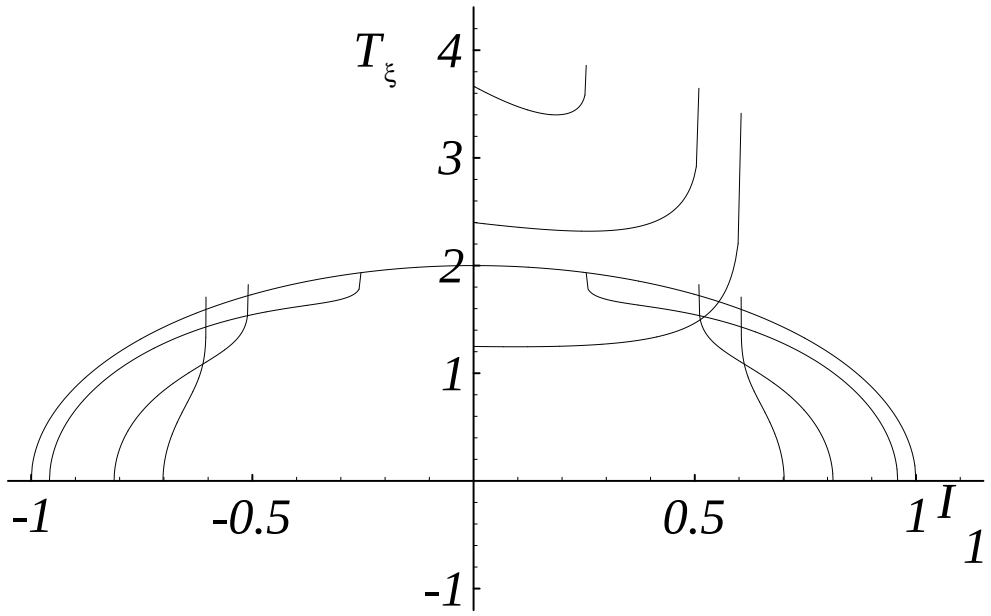

Figure 6: The period T_ξ of ξ-oscillations as a function of I_1. The values of a are the same as in Fig. 4.

4 Prolate ellipsoids

The prolate ellipsoid

$$x^2 \;+\; \frac{y^2+z^2}{1-a^2} \;=\; 1 \qquad (0 \le a < 1) \tag{41}$$

derives from the ellipse (15) via rotation about the x-axis. The corresponding rotational symmetry ensures the existence of a third constant of motion, namely, the x-component of the angular momentum. Determination of the actions is therefore no more difficult than in the planar case of an ellipse.

The coordinates (ξ, η, φ) are the natural extension of the elliptic coordinates of the previous section, φ being the angle of rotation about the x-axis. Their relation to the cartesian (x, y, z) is

$$(x, y, z) \;=\; \left(\frac{1}{a}\,\xi\eta,\; \frac{1}{a}\sqrt{(\xi^2-a^2)(a^2-\eta^2)}\,\cos\varphi,\; \frac{1}{a}\sqrt{(\xi^2-a^2)(a^2-\eta^2)}\,\sin\varphi\right)\;, \tag{42}$$

with coordinate ranges

$$a \le \xi \le 1\;, \qquad -a \le \eta \le a\;, \qquad 0 \le \varphi < 2\pi\;. \tag{43}$$

A single sheet of these coordinates covers the ellipsoid. The Hamiltonian is

$$H \;=\; \frac{1}{2}\,\frac{1}{\xi^2-\eta^2}\,\left((\xi^2-a^2){p_\xi}^2 \;+\; (a^2-\eta^2){p_\eta}^2\right) \;+\; \frac{a^2}{2}\,\frac{{p_\varphi}^2}{(\xi^2-a^2)(a^2-\eta^2)}\;, \tag{44}$$

and the elastic reflection at the boundary $\xi = 1$ is described by

$$(\xi, \eta, \varphi, p_\xi, p_\eta, p_\varphi) \to (\xi, \eta, \varphi, -p_\xi, p_\eta, p_\varphi)\;. \tag{45}$$

There are no further artificial reflections to be taken into account.

The system has three constants of motion: the total energy $H = E$, the angular momentum $p_\varphi = P_\varphi =: \sqrt{2E}\,l_\varphi$, and the separation constant $K = 2E\kappa^2$,

$$2E\xi^2 - (\xi^2-a^2){p_\xi}^2 - \frac{a^2\,{P_\varphi}^2}{\xi^2-a^2} \;=\; K\;, \tag{46}$$

$$2E\eta^2 + (a^2-\eta^2){p_\eta}^2 + \frac{a^2\,{P_\varphi}^2}{a^2-\eta^2} \;=\; K\;. \tag{47}$$

In the limit $a \to 0$, the elliptic coordinates reduce essentially to spherical coordinates, $(\xi, \eta, \varphi) \to (r, a\cos\vartheta, \varphi)$, and the momenta $(p_\xi, p_\eta, p_\varphi) \to (p_r, -p_\vartheta/a\sin\vartheta, p_\varphi)$ correspondingly. The separation constant K becomes the total angular momentum squared, $K \to {p_\vartheta}^2 + {p_\varphi}^2/\sin^2\vartheta$.

The allowed ranges of l_φ and κ^2 are

$$-\sqrt{1-a^2} \le l_\varphi \le \sqrt{1-a^2} \qquad \text{and} \qquad {l_\varphi}^2 \le \kappa^2 \le 1 - \frac{a^2\,{l_\varphi}^2}{1-a^2}\;. \tag{48}$$

The physical interpretation of the extreme cases is the following. For $l_\varphi = \pm\sqrt{1-a^2}$, all energy is in the φ-motion, with $(\xi, \eta, p_\xi, p_\eta) = (1, 0, 0, 0)$; this means the particle slides along the ellipsoid's equator. The value of κ^2 is then necessarily equal to ${l_\varphi}^2$. In general, when $\kappa^2 = {l_\varphi}^2$, the motion is restricted to the equatorial plane, $(\eta, p_\eta) = (0, 0)$, with ξ-values in the range $a^2 + {l_\varphi}^2 \le \xi^2 \le 1$. The effect of a finite angular momentum l_φ is to keep the particle away from the x-axis. At the other extreme, when $\kappa^2 = 1 - a^2\,{l_\varphi}^2/(1-a^2)$, the motion is restricted to the ellipsoid's surface, $(\xi, p_\xi) = (1, 0)$, the values of η being confined to the range $\eta^2 \le a^2 + \kappa^2 - 1$. With ${l_\varphi}^2$ growing towards its maximum possible value $1 - a^2$, the geodesic motion takes place in an equatorial belt of decreasing width.

The invariant tori for given E, l_φ, and κ^2 are again the direct product of three circles, $\varphi \in S^1$ and two related circles in the (ξ, p_ξ)- and (η, p_η)-planes, obtained explicitly by solving Eqs. (46) and (47) for p_ξ and p_η:

$$ {p_\xi}^2 \;=\; 2E\,\frac{(\xi^2 - n_1^2)(\xi^2 - n_2^2)}{(\xi^2 - a^2)^2}\;, \qquad {p_\eta}^2 \;=\; 2E\,\frac{(n_1^2 - \eta^2)(n_2^2 - \eta^2)}{(a^2 - \eta^2)^2}\;, \tag{49} $$

where n_1 and n_2 are defined by

$$ n_{1,2}^2 \;=\; \frac{1}{2}\,\Big(a^2 + \kappa^2 \pm \sqrt{(a^2-\kappa^2)^2 + 4a^2{l_\varphi}^2}\;\Big) \quad \text{with} \quad 0 < n_2 < a < n_1 < 1\;. \tag{50} $$

Fig. 7 shows these tori for $a = 0.4$ and $l_\varphi = 0.4$. In contrast to the planar elliptical billiard (cf. Fig. 3), there is no separatrix here because the centrifugal potential keeps the motion away from the x-axis, for any $l_\varphi \neq 0$. There is no discontinuity in the types of motion any more; ξ and η coordinates both vary in an oscillatory manner.

The computation of actions is now straightforward. With an obvious definition for the integration paths C_φ, C_η, and C_ξ, we have

$$ \begin{aligned} I_1 \;\equiv\; \frac{I_\varphi}{\sqrt{2E}} \;&=\; \frac{1}{2\pi}\oint_{C_\varphi} \frac{p_\varphi}{\sqrt{2E}}\,d\varphi = l_\varphi \\ I_2 \;\equiv\; \frac{I_\eta}{\sqrt{2E}} \;&=\; \frac{1}{2\pi}\oint_{C_\eta} \frac{p_\eta}{\sqrt{2E}}\,d\eta \;=\; \frac{2}{\pi}\int_0^{n_2} \frac{\sqrt{(n_1^2-\eta^2)(n_2^2-\eta^2)}}{a^2-\eta^2}\,d\eta \\ I_3 \;\equiv\; \frac{I_\xi}{\sqrt{2E}} \;&=\; \frac{1}{2\pi}\oint_{C_\xi} \frac{p_\xi}{\sqrt{2E}}\,d\xi \;=\; \frac{1}{\pi}\int_{n_1}^{1} \frac{\sqrt{(\xi^2-n_1^2)(\xi^2-n_2^2)}}{\xi^2-a^2}\,d\xi \end{aligned} \tag{51} $$

Using standard methods, and notation, as described in [14], the integrals I_2 and I_3 can be expressed in terms of elliptic integrals. Being a complete integral, I_2 is the simpler one of the two. With

$$ k = \frac{n_2}{n_1} \qquad \text{and} \qquad \alpha^2 = \frac{n_2^2}{a^2}\;, \tag{52} $$

we find

$$ I_2 \;=\; \frac{2}{\pi}\,\Big((\kappa^2 - n_1^2)\,\mathcal{K}(k) \;+\; n_1^2\,\mathcal{E}(k) \;-\; {l_\varphi}^2\,\Pi(\alpha^2, k)\Big)\;. \tag{53} $$

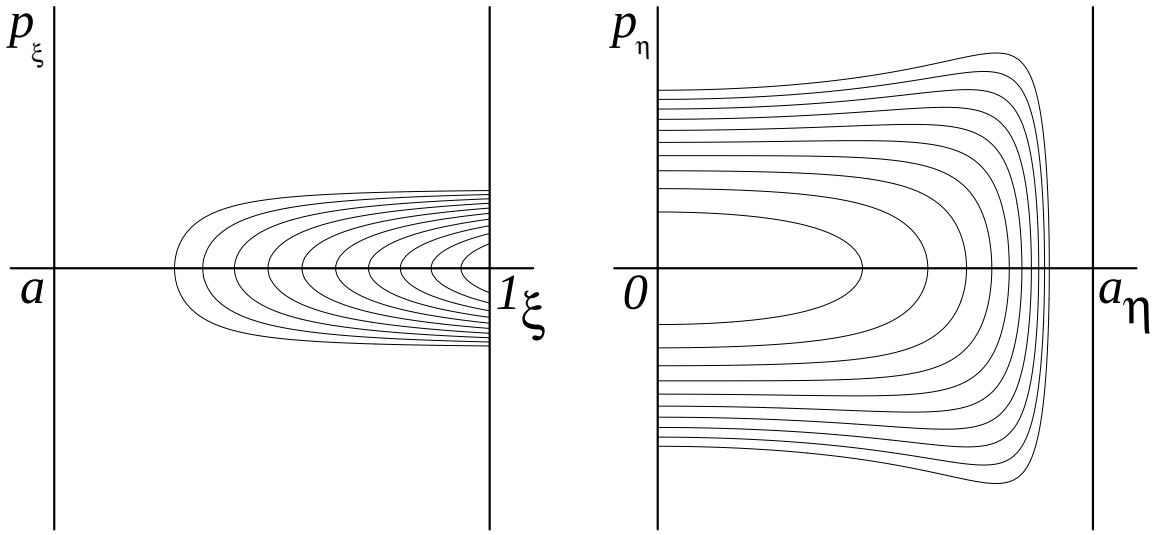

Figure 7: Phase portrait of billiard motion in a prolate ellipsoid. $a = 0.4$, $l_\varphi = 0.4$. Equidistant values of κ^2 have been chose. Left: intersection of invariant tori with the (ξ, p_ξ)-plane; right: intersection of invariant tori with the (η, p_η)-plane. There is no separatrix.

where $\Pi(\alpha^2, k)$ is a complete elliptic integral of the third kind. Numerically it is advantageous to have a negative parameter α^2, which may be achieved by means of the addition theorem (Eq.(117.03) in [14])

$$\Pi(\alpha^2, k) = \frac{\alpha^2}{1-\alpha^2}\,\frac{1-k^2}{\alpha^2-k^2}\,\Pi(-\beta^2, k) - \frac{k^2}{\alpha^2-k^2}\,\mathcal{K}(k) \quad \text{with} \quad \beta^2 = \frac{k^2-\alpha^2}{1-\alpha^2}\ . \tag{54}$$

With α^2 and k as given in Eq. (52), we have

$$\beta^2 = \frac{n_1^2 - a^2}{a^2 - n_2^2}\,k^2\ . \tag{55}$$

The action I_η is thus given by

$$\begin{aligned} I_2 \;=\; \frac{2}{\pi n_1}\,\Bigg(& (\kappa^2 - n_1^2 + \frac{a^2\, l_\varphi^{\,2}}{n_1^2 - a^2})\,\mathcal{K}(k) \;+\; n_1^2 \mathcal{E}(k) \\ & - \frac{a^2\, l_\varphi^{\,2}(n_1^2 - n_2^2)}{(n_1^2 - a^2)(a^2 - n_2^2)} \Pi(-\beta^2, k)\Bigg) \end{aligned} \tag{56}$$

The action I_ξ involves incomplete elliptic integrals, with parameters

$$k = \frac{n_2}{n_1}\ , \qquad \gamma^2 = \frac{a^2 - n_2^2}{n_1^2 - a^2}\ , \qquad \sin^2\chi = \frac{1-n_1^2}{1-n_2^2}\ ; \tag{57}$$

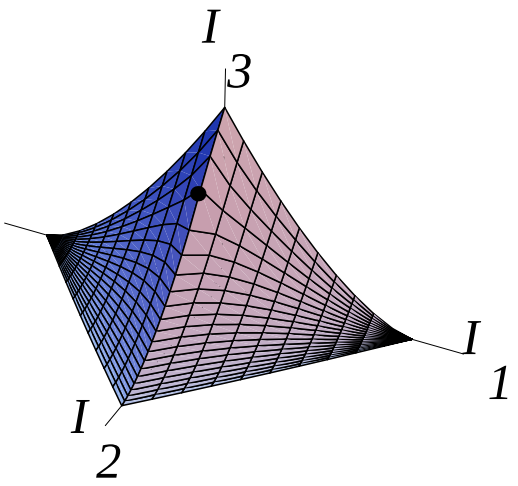

Figure 8: Energy surface for billiard motion in a prolate ellipsoid. I_1 is the angular momentum component with respect to the symmetry axis; I_2 is the action of η-motion; I_3 is the action of ξ-motion. The black dot at $(I_1, I_2, I_3) = (0, 2a/\pi, (1-a)/\pi)$ marks the singular point which corresponds to motion through the foci.

the result is

$$\begin{aligned} I_3 \;=\; \frac{1}{\pi n_1}\,\Bigg(& (-\kappa^2 + n_1^2 + \frac{a^2\, l_\varphi^{\,2}}{a^2 - n_2^2})\;\mathcal{F}(\chi,k) \;-\; n_1^2 \mathcal{E}(\chi,k) \\ & - \frac{a^2\, l_\varphi^{\,2}(n_1^2 - n_2^2)}{(n_1^2 - a^2)(a^2 - n_2^2)} \Pi(\chi, -\gamma^2, k) \;+\; n_1 \sin\chi \;\Bigg) \end{aligned} \tag{58}$$

Fig. 8 gives a graphical illustration of the energy surface in action space. It resembles the half tent structure for the spherical billiard, cf. Fig. 1, and indeed, for $I_2 = 0$ the two figures coincide up to a scaling factor $\sqrt{1-a^2}$ in the actions I_1 and I_3 which accounts for the radius of the ellipsoid's equator.

The condition $I_\eta = 0$ is characteristic of motion confined to the equatorial plane, i. e., it describes the situation of a planar circular billiard. It is obtained with $(\eta, p_\eta) = (0, 0)$ which implies $\kappa^2 = l_\varphi^{\,2}$, $n_2 = 0$, $n_1^2 = a^2 + \kappa^2$. The parameters in the elliptic integrals are therefore

$$k = 0\;, \quad \gamma^2 = \frac{a^2}{\kappa^2}\;, \quad \text{and} \quad \sin^2\chi = 1 - n_1^2 = (1-a^2)(1 - \frac{l_\varphi^{\,2}}{1-a^2}) =: (1-a^2)\sin^2\phi \tag{59}$$

Using the identities $\mathcal{F}(\chi, 0) = \mathcal{E}(\chi, 0) = \chi$ and

$$\Pi(\chi, -\gamma^2, 0) \;=\; \frac{1}{\sqrt{1+\gamma^2}} \arctan\left(\sqrt{1+\gamma^2}\;\tan\chi\right)\;, \tag{60}$$

we find

$$I_\xi \;=\; \frac{\sqrt{2E}}{\pi}\,(\sin\chi - |l_\varphi|\,\phi) \;=\; \frac{\sqrt{2E(1-a^2)}}{\pi}\,(\sin\phi - \phi\,|\cos\phi|) \tag{61}$$

which agrees with the result for I_3 in Eq. (4) if the radius of the equatorial circle is taken into account.

Another special situation occurs for $I_\varphi \to 0$. This condition characterizes the limiting case of a planar elliptic billiard. We should expect it to coincide with Fig. 4, but at first glance it doesn't. The reason is that the prolate ellipsoid derives from rotation of only half the planar elliptic billiard about the x-axis; the other half is generated by rotation with angle π. As a consequence, the $I_\eta < 0$ part of Fig. 4 disappears, and I_ξ is reduced by a factor 2 in the small I_η regime. This makes for a continuous curve I_η vs. I_ξ, for $I_\varphi = 0$, with only a weak singularity (logarithmic divergence of the derivative) at the separatrix $I_\eta/\sqrt{2E} = I_2 = 2a/\pi$. Analytically it is straightforward to derive the actions of Sec. 3 from Eqs. (53) and (58). For type I orbits, or $\kappa^2 > a^2$, we have $n_1^2 = \kappa^2$, and $n_2^2 = a^2$; for type II orbits, it's the other way round. In any case, Eqs. (23), (25), and (29), (30) follow immediately.

If the lines $I_\eta = 0$ and $I_\varphi \to 0$ of the energy surface in Fig. 8 could be identified as familiar cases of planar billiards, the situation is different for $I_\xi = 0$. This condition characterizes geodesic motion on the ellipsoid's surface, $(\xi, p_\xi) = (1, 0)$. Using

$$\kappa^2 = 1 - \frac{a^2\, {l_\varphi}^2}{1-a^2}\,, \quad n_1 = 1\,, \quad n_2^2 = a^2 + \kappa^2 - 1 = k^2\,, \quad \alpha^2 = \frac{n_2^2}{a^2}\,, \quad \beta^2 = \frac{1-a^2}{1-\kappa^2}\,n_2^2\,, \tag{62}$$

we can reduce Eq. (53) to

$$I_2 \;=\; \frac{2}{\pi}\,\left(-\,\frac{a^2\,{l_\varphi}^2}{1-a^2}\,\mathcal{K}(k) \;+\; \mathcal{E}(k) \;-\; {l_\varphi}^2\,\Pi\left(1 - \frac{{l_\varphi}^2}{1-a^2}, k\right)\right)\,, \tag{63}$$

and Eq. (56) to

$$I_2 \;=\; \frac{2}{\pi}\,\Big(\mathcal{E}(k) \;-\; (1-k^2)\Pi(-\beta^2, k)\Big)\,. \tag{64}$$

The first of these two equivalent results is best suited to recover the result $I_\eta/\sqrt{2E} = 2\mathcal{E}(a)/\pi$ for motion along an ellipse $\xi = 1$, $\varphi =$const, cf. Eq. (23) in the limit $\kappa = 1$. The second formula (64) gives the limit $I_\eta = 0$ for circular motion more easily, as $k = \beta = 0$ and $\mathcal{E}(0) = \Pi(0, 0) = \pi/2$.

There is a 1–1 correspondence of points $(I_\varphi, I_\eta, I_\xi)$ on the energy surface shown in Fig. 8, and the invariant 3-tori characterized by the constants of motion (E, l_φ, κ). If one of the actions vanishes, the tori are critical or foliated by 2-tori. If two actions vanish simultaneously, they degenerate further. This is the case for

1. $I_\varphi = I_\eta = 0$, $I_\xi/\sqrt{2E} = \sqrt{1-a^2}/\pi$: linear oscillatory motion in the equatorial (y, z)-plane;

2. $I_\varphi = I_\xi = 0$, $I_\eta/\sqrt{2E} = 2\mathcal{E}(a)/\pi$: geodesic motion along an ellipse $\xi = 1$, $\varphi =$const;

3. $I_\xi = I_\eta = 0$, $I_\varphi/\sqrt{2E} = \pm\sqrt{1-a^2}$: geodesic motion along the equator, the direction depending on the sign of I_φ.

There is one more critical 1-torus, corresponding to an unstable periodic orbit: it corresponds to the separatrix in the case of a planar elliptic billiard, $(I_\varphi, I_\eta, I_\xi)/\sqrt{2E} = (0, 2a/\pi, (1-a)/\pi)$. The motion is linear oscillation along the symmetry axis of the ellipsoid. But note that in this particular case, the constants $(E, l_\varphi = 0, \kappa = a)$ do not only specify this critical torus but also its stable and unstable manifolds.

5 Oblate ellipsoids

The oblate ellipsoid

$$x^2 \; + \; \frac{y^2}{1-a^2} \; + \; z^2 \; = \; 1 \qquad (0 \le a < 1) \tag{65}$$

derives from the ellipse (15) via rotation about the y-axis. The foci thereby form a circle of radius a in the (x,z)-plane, and this must be expected to have a stronger impact on the shape of the energy surface than did the two focal points on the x-axis of the prolate ellipsoid in Sec. 4. Indeed it will be seen that instead of just one singular point there appears a singular line dividing the energy surface into two parts.

The rotational symmetry with respect to the y-axis implies again the constancy of the corresponding angular momentum. Computation of the actions thus does not lead beyond Jacobi's elliptic integrals.

We adapt the coordinates (ξ,η,φ) to the new rotational symmetry:

$$(x,y,z) \; = \; \left(\frac{1}{a}\,\xi\eta \, \cos\varphi, \; \pm\frac{1}{a}\sqrt{(\xi^2-a^2)(a^2-\eta^2)}\,, \; \frac{1}{a}\,\xi\eta \, \sin\varphi \right) \; , \tag{66}$$

with ranges

$$a \le \xi \le 1 \; , \qquad 0 \le \eta \le a \; , \qquad 0 \le \varphi < 2\pi \; , \tag{67}$$

and two sheets for the $y > 0$ and $y < 0$ halves of the ellipsoid.

The Hamiltonian is

$$H \; = \; \frac{1}{2} \, \frac{1}{\xi^2-\eta^2} \, \left((\xi^2-a^2) {p_\xi}^2 \; + \; (a^2-\eta^2) {p_\eta}^2 \; + \; a^2 \, {p_\varphi}^2 \, (\frac{1}{\eta^2} - \frac{1}{\xi^2}) \right) \; , \tag{68}$$

and the elastic reflection condition at the boundary $\xi = 1$ is the same as in Eq. (45). In addition, we have formal reflections whenever the boundaries $\xi = a$ or $\eta = a$ of the coordinate sheets are reached and a transition to the other sheet takes place. The situation is similar to the case of the planar elliptic billiard, except for the sheets here being only half the size in η. The other half is generated by the rotation.

The three constants of motion are again the total energy $H = E$, the angular momentum $p_\varphi = P_\varphi =: \sqrt{2E}\, l_\varphi$, and the separation constant $K = 2E\kappa^2$,

$$2E\xi^2 - (\xi^2-a^2) {p_\xi}^2 + \frac{a^2 \, {P_\varphi}^2}{\xi^2} \; = \; K \; , \tag{69}$$

$$2E\eta^2 + (a^2-\eta^2) {p_\eta}^2 + \frac{a^2 \, {P_\varphi}^2}{\eta^2} \; = \; K \; . \tag{70}$$

The limit $a \to 0$ in this case gives $(\xi,\eta,\varphi) \to (r, a\sin\vartheta, \varphi)$, for the coordinates, and for the momenta $(p_\xi, p_\eta, p_\varphi) \to (p_r, p_\vartheta/a\cos\vartheta, p_\varphi)$. But the separation constant K becomes again the square of the total angular momentum.

Analysis of the allowed parameter range for l_φ and κ^2 gives the following. First, it is easy to see that l_φ is restricted by

$$-1 \leq l_\varphi \leq 1 \ , \tag{71}$$

the two extreme cases ${l_\varphi}^2 = 1$ corresponding to motion along the ellipsoid's equator: $(\xi, \eta, p_\xi, p_\eta) = (1, a, 0, 0)$. Eqs. (69) and (70) then imply $\kappa^2 = 1 + a^2$. For ${l_\varphi}^2 < 1$, there is a range of possible κ^2-values, depending on ${l_\varphi}^2$,

$$\kappa^2_{min} \leq \kappa^2 \leq \kappa^2_{max} \ . \tag{72}$$

As in the prolate ellipsoid, κ^2 assumes its maximum for geodesic motion on the surface, i. e., for $(\xi, p_\xi) = (1, 0)$. This corresponds to

$$\kappa^2_{max} \ = \ 1 + a^2 \, {l_\varphi}^2 \tag{73}$$

by Eq. (69), and an η-range $a^2 \, {l_\varphi}^2 \leq \eta^2 \leq a^2$ by Eq. (70). The discussion of κ^2_{min} is a little more involved, as it depends on whether ${l_\varphi}^2$ is smaller or larger than a^2. Considering Eq. (70) for $p_\eta = 0$, we may look for the smallest possible κ^2 by varying η^2. This is found to occur at $\eta^2 = \eta^2_{min} = a|l_\varphi|$, with $\kappa^2_{min} = 2a|l_\varphi|$. But note that $\eta^2_{min} < a^2$, as required by the coordinate range (67), only if ${l_\varphi}^2 < a^2$. For ${l_\varphi}^2 > a^2$, on the other hand, κ^2 assumes its minimum if η takes on its highest possible value a, together with p_η being zero. This implies $\kappa^2_{min} = a^2 + {l_\varphi}^2$. To sum up, the smallest possible κ^2 at given l_φ is

$$\kappa^2_{min} \ = \ \begin{cases} 2a|l_\varphi| & \text{if} \quad {l_\varphi}^2 \leq a^2 \ , \\ a^2 + {l_\varphi}^2 & \text{if} \quad {l_\varphi}^2 \geq a^2 \ . \end{cases} \tag{74}$$

What is the motion like if $\kappa^2 = \kappa^2_{min}$? For ${l_\varphi}^2 > a^2$, since $(\eta, p_\eta) = (a, 0)$, the motion takes place in the (x, z)-plane; this is the limit of a planar circular billiard, but with the further restriction that it stays outside the focal circle of radius a. For ${l_\varphi}^2 < a^2$, on the other hand, the motion takes place on the hyperboloid $\eta = \sqrt{a\,|l_\varphi|}$, approaching oscillation along the y-axis as $l_\varphi \to 0$.

But what about the planar circular billiard motion with small angular momentum, ${l_\varphi}^2 < a^2$? Its κ-value is given by $\kappa^2 = a^2 + {l_\varphi}^2$ which is larger than κ^2_{min} in this range of l^2, so it does not correspond to a stable orbit. In the limit as $l_\varphi \to 0$ it approaches the unstable periodic motion of the planar elliptical billiard. We will see in connection with Eqs. (86) - (88) that this motion marks the separatrix between the two major types: type I which crosses the (x, z)-plane outside the focal circle, and type II which crosses inside.

Let us consider examples of the two types of invariant tori in their projections on the (ξ, p_ξ)- and (η, p_η)-planes. From Eqs. (69) and (70) we obtain

$${p_\xi}^2 \ = \ 2E \, \frac{(\xi^2 - n_1^2)(\xi^2 - n_2^2)}{\xi^2 \, (\xi^2 - a^2)} \ , \qquad {p_\eta}^2 \ = \ 2E \, \frac{(n_1^2 - \eta^2)(\eta^2 - n_2^2)}{\eta^2 (a^2 - \eta^2)} \ , \tag{75}$$

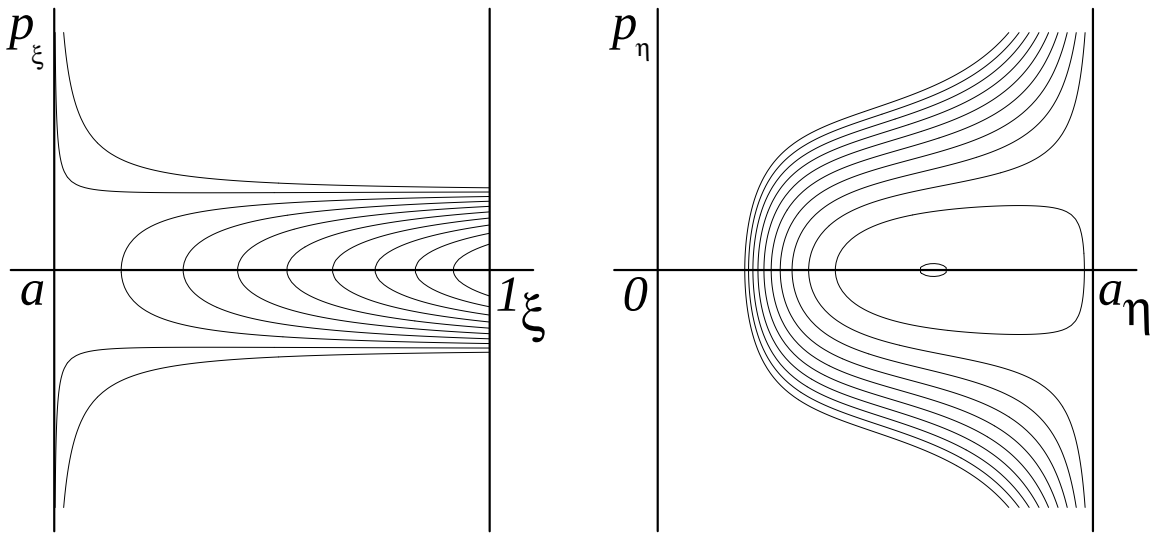

Figure 9: Phase portraits of billiard motion in an oblate ellipsoid. $a = 0.5$, $l_\varphi = 0.2$. Left: intersection of invariant tori with the (ξ, p_ξ)-plane; right: intersection of invariant tori with the (η, p_η)-plane. There are obviously two types of motion. Type I: motion where ξ never gets down to a, i. e., the inner circle is never reached; its stable center is geodesic motion on the ellipsoid, $\xi = 1$. Type II: motion where η never gets up to a, i. e., the outer ring is never reached; its stable center is motion on the hyperboloid $\eta^2 = a|l_\varphi|$. The separatrix between the two types consists of orbits that go through the focal circle, $\xi = \eta = a$.

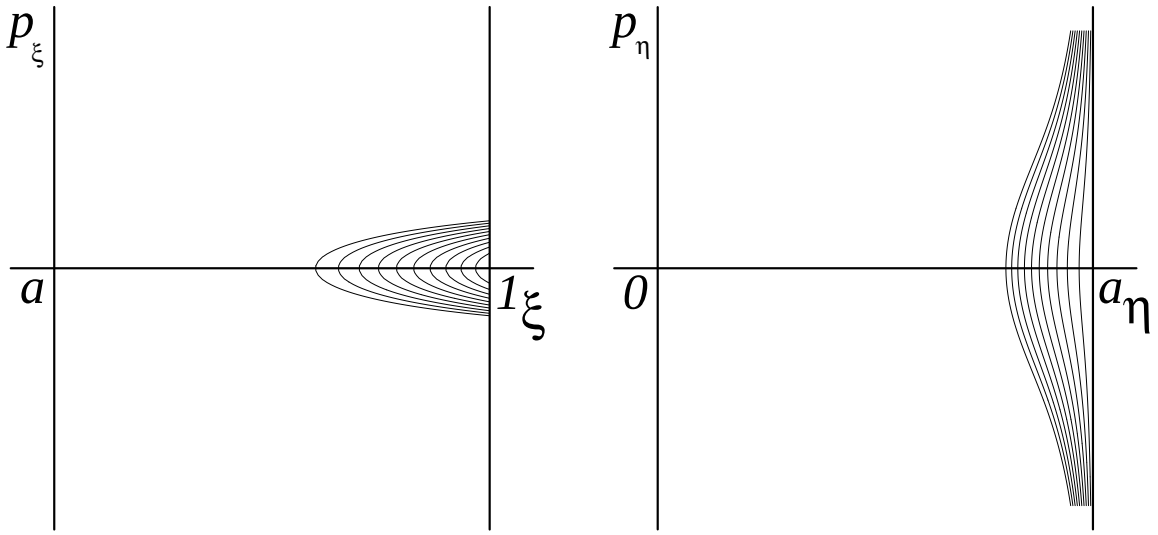

Figure 10: Phase portraits of billiard motion in an oblate ellipsoid. $a = 0.5$, $l_\varphi = 0.8$. Left: intersection of invariant tori with the (ξ, p_ξ)-plane; right: intersection of invariant tori with the (η, p_η)-plane. There is only type I motion, and no separatrix.

where n_1 and n_2 are defined by

$$n_{1,2}^2 \;=\; \frac{\kappa^2}{2} \pm \frac{1}{2}\,\sqrt{\kappa^4 - 4a^2\,l_\varphi^{\,2}} \quad \text{with} \quad 0 \le n_2^2 \le n_1^2 \le 1\ . \tag{76}$$

Figs. 9 and 10 give examples of the behavior at small and large angular momentum.

To compute the actions, we need to identify a set of fundamental paths C_φ, C_η, C_ξ around the invariant tori. This is different in the two cases of type I and II. Consider first type I tori where a complete period in ξ involves one loop from $\xi = n_1$ up to 1 and back to n_1, whereas the η-loop has to cover both coordinate sheets.

$$\begin{aligned}
I_1 \;\equiv\; \frac{I_\varphi}{\sqrt{2E}} \;&=\; \frac{1}{2\pi}\oint_{C_\varphi} \frac{p_\varphi}{\sqrt{2E}}\,d\varphi = l_\varphi \\
I_2 \;\equiv\; \frac{I_\eta}{\sqrt{2E}} \;&=\; \frac{1}{2\pi}\oint_{C_\eta} \frac{p_\eta}{\sqrt{2E}}\,d\eta \;=\; \frac{2}{\pi}\int_{n_2}^{a} \sqrt{\frac{(n_1^2-\eta^2)(\eta^2-n_2^2)}{a^2-\eta^2}}\;\frac{d\eta}{\eta} \\
I_3 \;\equiv\; \frac{I_\xi}{\sqrt{2E}} \;&=\; \frac{1}{2\pi}\oint_{C_\xi} \frac{p_\xi}{\sqrt{2E}}\,d\xi \;=\; \frac{1}{\pi}\int_{n_1}^{1} \sqrt{\frac{(\xi^2-n_1^2)(\xi^2-n_2^2)}{\xi^2-a^2}}\;\frac{d\xi}{\xi}
\end{aligned} \tag{77}$$

Evaluation of the integrals leads to the following results. With

$$k^2 = \frac{a^2-n_2^2}{n_1^2-n_2^2}\ , \qquad \alpha^2 = \frac{n_1^2}{a^2}k^2\ , \qquad \sin^2\psi = \frac{1-n_1^2}{1-a^2}\ , \tag{78}$$

the η-action is

$$I_2 \;=\; \frac{2}{\pi}\,\sqrt{n_1^2-n_2^2}\;\left(\mathcal{E}(k)\;-\;(1-k^2)\,\frac{n_2^2}{a^2}\,\Pi(\alpha^2,k)\right)\;, \tag{79}$$

whereas I_ξ is given in terms of incomplete elliptic integrals,

$$I_3=\frac{1}{\pi}\,(1-k^2)\,\sqrt{n_1^2-n_2^2}\;\left(\Pi(\psi,1,k)-\frac{n_2^2}{a^2}\,\Pi(\psi,\frac{a^2}{n_1^2},k)-(1-\frac{n_2^2}{a^2})\,\mathcal{F}(\psi,k)\right)\;. \tag{80}$$

In type II tori, the path C_η performs one η-loop from n_2 up to n_1 and back to n_2, whereas C_ξ involves two ξ-loops from a to 1 and back. The result for the actions involves parameters

$$k^2=\frac{n_1^2-n_2^2}{a^2-n_2^2}\;,\qquad \beta^2=\frac{a^2}{n_1^2}k^2\;,\qquad \sin^2\chi=\frac{1-a^2}{1-n_1^2}\;. \tag{81}$$

We find

$$I_2 \;=\; \frac{1}{\pi}\,\sqrt{a^2-n_2^2}\;\left(\mathcal{E}(k)\;-\;(1-\frac{n_1^2}{a^2})\,\mathcal{K}(k)\;-\;(1-k^2)\,\frac{n_2^2}{a^2}\,\Pi(\beta^2,k)\right)\;, \tag{82}$$

and

$$I_3 \;=\; \frac{2}{\pi}\,(1-k^2)\,\sqrt{a^2-n_2^2}\;\left(\Pi(\chi,1,k)\;-\;\frac{n_2^2}{a^2}\,\Pi(\chi,\frac{n_1^2}{a^2},k)\right)\;. \tag{83}$$

Fig. 11 shows a typical energy surface of this kind. It consists of two discontinuous parts, representing type I and type II motion respectively. Type I occurs at large I_η and small I_ξ; at the transition towards type II, I_η is reduced by a factor 1/2 whereas I_ξ is enlarged by a factor of 2.

Let us discuss the special cases of stable critical tori, beginning with $I_\eta = 0$. This is different for $l_\varphi^{\,2} > a^2$ (type I) and $l_\varphi^{\,2} < a^2$ (type II). For type I, we get $I_\eta = 0$ if $(\eta, p_\eta) = (a, 0)$ and therefore $\kappa^2 = a^2 + l_\varphi^{\,2}$, $n_1^2 = l_\varphi^{\,2}$, $n_2^2 = a^2$. The parameters of the elliptic integrals are $k^2 = \alpha^2 = 0$ and $\sin^2\psi = (1 - l_\varphi^{\,2})/(1 - a^2)$. Using the limiting behavior of elliptic integrals, $\Pi(\psi, 1, 0) = \tan\psi$ and $\Pi(\psi, N, 0) = \arctan\,(\sqrt{1-N}\,\tan\psi)/\sqrt{1-N}$, and defining the angle ϕ by $\cos\phi = l_\varphi$, we get the familiar result

$$I_\xi \;=\; \frac{\sqrt{2E}}{\pi}\,(\sin\phi - \phi\,|\cos\phi|) \qquad\qquad (l_\varphi^2 = \cos^2\phi > a^2) \tag{84}$$

for planar circular billiards, cf. Eq. (4). For $l_\varphi^{\,2} < a^2$, or type II motion, on the other hand, the action I_η vanishes if $(\eta, p_\eta) = (\sqrt{a l_\varphi}\,, 0)$ and thus $\kappa^2 = 2a|l_\varphi|$, $n_1^2 = n_2^2 = a|l_\varphi|$. The parameters of the elliptic integrals are $k^2 = \beta^2 = 0$ and $\sin^2\chi = (1 - a^2)/(1 - a|l_\varphi|)$. Using again the appropriate limiting formulas for $\Pi(\chi, N, 0)$, we find

$$I_3 \;=\; \frac{2}{\pi}\,\left(\sqrt{1-a^2}\;-|l_\varphi|\,\sqrt{\frac{a}{a+|l_\varphi|}}\;\arctan\sqrt{\frac{(a+|l_\varphi|)(1-a^2)}{a^3}}\;\right) \qquad (l_\varphi^2 < a^2)\;. \tag{85}$$

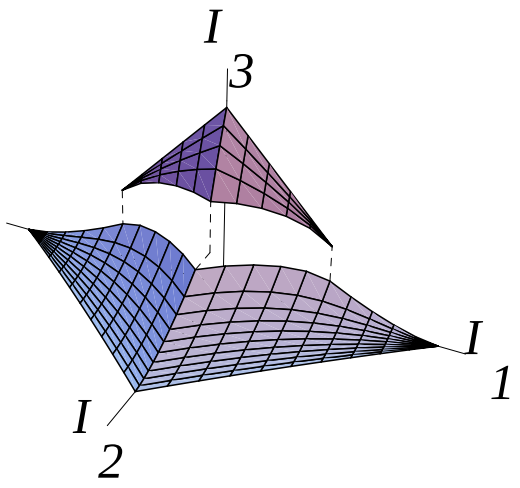

Figure 11: Energy surface for billiard motion in an oblate ellipsoid. I_1 is the angular momentum component with respect to the symmetry axis; I_2 is the action of η-motion; I_3 is the action of ξ-motion. The surface consists of two disconnected sheets, separated along the line of unstable motion in the equatorial plane with angular momentum $l_\varphi^2 < a^2$.

This is the action of motion restricted to the surface of a hyperboloid $\eta^2 = a|l_\varphi|$ which in the limit $l_\varphi = 0$ reduces to stable oscillatory motion along the y-axis.

The orbits of the planar circular billiard which cross the focal circle, ${l_\varphi}^2 < a^2$, are not characterized by $I_\eta = 0$. Rather they produce here the separatrix. Their parametrization is different for the parts inside and outside that circle. The inner part is given by $\xi = a$ and ${l_\varphi}^2 \le \eta^2 \le a^2$, the outer part by $\eta = a$ and $a^2 \le \xi^2 \le 1$. The corresponding action integrals are elementary, the only point that needs some caution being the choice of paths that give the correct limits in the two cases of type I and type II orbits. With

$$I_< \;:=\; \frac{1}{\pi}\, a\, (\sin\psi - \psi\,|\cos\psi|) \quad \text{and} \quad I_> \;:=\; \frac{1}{\pi}\,(\sin\phi - \phi\,|\cos\phi|) \;-\; I_<\;, \tag{86}$$

where

$$\cos\phi = l_\varphi \qquad \text{and} \qquad \cos\psi = \frac{l_\varphi}{a}\;, \tag{87}$$

we have

$$I_2 \;=\; \begin{cases} 2I_< & \text{type I} \\ I_< & \text{type II} \end{cases} \qquad \text{and} \qquad I_3 \;=\; \begin{cases} I_> & \text{type I} \\ 2I_> & \text{type II} \end{cases}\;. \tag{88}$$

ψ is the angle between the trajectory and the tangent to the focal circle at the point of crossing. It is 0 for ${l_\varphi}^2 = a^2$ so that $I_{in} = 0$, and grows to $\pi/2$ when $\phi = \pi/2$; then we have $I_{in}/\sqrt{2E} = a/\pi$ and $I_{out}/\sqrt{2E} = (1-a)/\pi$.

In the limit $I_\varphi = 0$, we find from Eq. (76) $n_1 = \kappa$ and $n_2 = 0$. For type I motion, $\kappa > a$, this implies $k^2 = a^2/\kappa^2$, $\alpha^2 = 1$, and $\sin^2\psi = (1-\kappa^2)/(1-a^2)$; the results (79), (80) reduce to Eqs. (23) and (25) respectively. For $\kappa < a$, or type II motion, we have $k^2 = \kappa^2/a^2$, $\beta^2 = 1$, and $\sin^2\chi = (1-a^2)/(1-\kappa^2)$. Eqs. (82) then gives half the value of I_η according to Eq. (29), and (83) reduces to the I_ξ from Eq. (30).

Finally, when $I_\xi = 0$ we have geodesic motion on the surface of the ellipsoid, $(\xi, p_\xi) = (1, 0)$, and

$$\kappa^2 = 1 + a^2 {l_\varphi}^2 \ , \quad n_1 = 1 \ , \quad n_2^2 = a^2 \, {l_\varphi}^2 \ , \quad k^2 = \frac{a^2(1-{l_\varphi}^2)}{1-a^2{l_\varphi}^2} \ , \quad \alpha^2 = \frac{k^2}{a^2} \ , \tag{89}$$

so that Eq. (79) reduces to

$$I_\eta \ = \ \frac{2\sqrt{2E}}{\pi} \ \left(\sqrt{1-a^2{l_\varphi}^2} \ \mathcal{E}(k) \ - \ \frac{(1-a^2)\,{l_\varphi}^2}{\sqrt{1-a^2{l_\varphi}^2}} \, \Pi(\alpha^2, k) \right) \ . \tag{90}$$

The periodic orbits corresponding to the corners of the energy surface are the following:

1. $I_\varphi = I_\eta = 0$, $I_\xi/\sqrt{2E} = 2\sqrt{1-a^2}\,/\pi$: linear oscillatory motion along the y-axis;
2. $I_\varphi = I_\xi = 0$, $I_\eta/\sqrt{2E} = 2\mathcal{E}(a)/\pi$: geodesic motion along an ellipse $\xi = 1$, $\varphi =$const;
3. $I_\xi = I_\eta = 0$, $I_\varphi/\sqrt{2E} = \pm 1$: geodesic motion along the equator, the direction depending on the sign of I_φ.

6 Outlook

Jacobi's 26th lecture on *Dynamics* [17] is devoted to a discussion of elliptic coordinates for n-dimensional quadrics. It starts with the phrase: "Die Hauptschwierigkeit bei der Integration gegebener Differentialgleichungen scheint in der Einführung der richtigen Variablen zu bestehen, zu deren Auffindung es keine allgemeine Regel giebt."[4] It was one of his many great achievements to have found such a set of variables, and thereby to solve the problem of finding the geodesics on an n-dimensional ellipsoid.

In the special case of three dimensions it has turned out that Jacobi's elliptic coordinates and their various limiting cases (of which there are ten different, including rectangular, cylindrical, spherical, conical, and paraboloidal coordinates) are the only coordinates that allow separation of the Hamiltonian of free motion, and correspondingly in wave mechanics, of the Laplacian operator [2]. The key to Jacobi's success was the mutual orthogonality of sets of confocal quadrics of which he remarks with some pride on page 208 of [17]: "Die Sätze über confocale Oberflächen zweiten Grades ... gehören zu den merkwürdigsten der analytischen Geometrie; ich habe einige der wichtigsten ... zuerst bekannt gemacht."[5]

The general three dimensional ellipsoid

$$x^2 \;+\; \frac{y^2}{1-b^2} \;+\; \frac{z^2}{1-a^2} \;=\; 1 \qquad (0 \le b \le a < 1) \tag{91}$$

is conveniently described by coordinates (ξ, η, ζ) whose relation to (x, y, z) is the following:

$$(x, y, z) = \left(\frac{\xi\eta\zeta}{ab}\,,\; \frac{\sqrt{(\xi^2-b^2)(\eta^2-b^2)(b^2-\zeta^2)}}{b\sqrt{a^2-b^2}}\,,\; \frac{\sqrt{(\xi^2-a^2)(a^2-\eta^2)(a^2-\zeta^2)}}{a\sqrt{a^2-b^2}} \right) \tag{92}$$

with coordinate ranges

$$0 \le \zeta \le b \le \eta \le a \le \xi \le 1\ . \tag{93}$$

Surfaces ξ =const are confocal ellipsoids, i. e., their sections with the (x, y)-plane are ellipses with foci at $(x, y) = (b, 0)$; their sections with the (x, z)-plane are ellipses with foci at $(x, z) = (a, 0)$; and their sections with the (y, z)-plane are ellipses with foci at $(y, z) = (\sqrt{a^2-b^2}, 0)$.

Surfaces η =const are confocal one-sheet hyperboloids, i. e., their sections with the (x, y)-plane are ellipses with foci at $(x, y) = (b, 0)$; their sections with the (x, z)-plane are hyperbolas with foci at $(x, z) = (a, 0)$; and their sections with the (y, z)-plane are hyperbolas with foci at $(y, z) = (\sqrt{a^2-b^2}, 0)$.

Surfaces ζ =const are confocal two-sheet hyperboloids, i. e., their sections with the (x, y)-plane are hyperbolas with foci at $(x, y) = (b, 0)$; their sections with the (x, z)-plane

[4] "The main difficulty with integrating a given set of differential equations seems to be the introduction of the right variables for which there is no general rule."

[5] "The theorems on confocal surfaces of second degree ... are among the most noteworthy in analytical geometry; I was first to have made known some of the most important ..."

are hyperbolas with foci at $(x,z) = (a,0)$; and they don't have intersections with the (y,z)-plane.

As we shall not derive explicit results in this general case, we ignore here the question of the number of coordinate sheets needed to cover the ellipsoid and particular tori.

The Hamiltonian H of free motion inside the ellipsoid $\xi = 1$ is easily computed,

$$2H \;=\; \frac{(\xi^2-a^2)(\xi^2-b^2)}{(\xi^2-\eta^2)(\xi^2-\zeta^2)}\,{p_\xi}^2 \;+\; \frac{(a^2-\eta^2)(\eta^2-b^2)}{(\xi^2-\eta^2)(\eta^2-\zeta^2)}\,{p_\eta}^2 \;+\; \frac{(a^2-\zeta^2)(b^2-\zeta^2)}{(\xi^2-\zeta^2)(\eta^2-\zeta^2)}\,{p_\zeta}^2 \quad (94)$$

and the elastic reflection at the boundary $\xi = 1$ is described by

$$(\xi,\eta,\zeta,p_\xi,p_\eta,p_\zeta) \to (\xi,\eta,\zeta,-p_\xi,p_\eta,p_\zeta)\ . \quad (95)$$

The separation of variables is done in two steps, as there are two separation constants k_1 and k_2. The result can be expressed in terms of the three projections of invariant tori on the (ξ,ψ)-, (η,p_η)-, and (ζ,p_ζ)-planes respectively:

$${p_\xi}^2 \;=\; 2E\,\frac{\xi^4-k_1\xi^2-k_2}{(\xi^2-a^2)(\xi^2-b^2)}\ , \quad (96)$$

$${p_\eta}^2 \;=\; 2E\,\frac{-\eta^4+k_1\eta^2+k_2}{(a^2-\eta^2)(\eta^2-b^2)}\ , \quad (97)$$

$${p_\zeta}^2 \;=\; 2E\,\frac{\zeta^4-k_1\zeta^2-k_2}{(a^2-\zeta^2)(b^2-\zeta^2)}\ . \quad (98)$$

Once this separation is achieved, the computation of actions is straightforward – in principle. We leave it for future work, or invite the reader to do it as an extended exercise. The task involves two steps. First, the scheme of bifurcations, or phase diagram in (k_1,k_2)-parameter space, must be established, and second, hyperelliptic integrals must be evaluated. The first part requires nothing more than an elementary discussion of the various possible ways in which the zeroes of the polynomial $P(t) = t^2 - k_1 t - k_2$ can be located in relation to a^2 and b^2. The evaluation of hyperelliptic integrals must be done numerically. It will be interesting to see how the energy surfaces come out to look like.

We remark at the end that with the same tools a number of further problems can be settled [5]. First, the billiard boundary need not be the ellipsoid $\xi = 1$; it could be any region bounded by surfaces ξ =const, η =const, and ζ =const. Second, as already noted by Jacobi, the motion need not be free. A harmonic potential with center at the origin may be added without spoiling the integrability. This introduces an interesting energy dependence of the energy surfaces, starting with harmonic oscillator behavior at low energy, and ending with the surfaces discussed here, as energy tends to infinity. The bifurcation scheme in $(E,k_1,k_2;a,b)$-parameter space may be expected to exhibit similar complexity as in the famous Kovalevskaya case of rigid body dynamics [18], [19], [20], [12]. The third generalization concerns the number of dimensions; it is remarkable, and was also known to Jacobi, that his separation scheme works in D-dimensional ellipsoids for any D.

References

[1] L. Dirichlet. Gedächtnisrede auf Carl Gustav Jacob Jacobi. In C. W. Borchardt, editor, *C. G. J. Jacobi's Gesammelte Werke I*, pages 3–28. Chelsea, New York, 1969.

[2] P. M. Morse and H. Feshbach. *Methods of Theoretical Physics*. McGraw-Hill, New York, Toronto, London, 1953.

[3] F. Klein and A. Sommerfeld. *Über die Theorie des Kreisels*. Teubner-Verlag, Leipzig, 1910.

[4] M. V. Berry. Regularity and chaos in classical mechanics, illustrated by three deformations of a circular billiard. *Eur. J. Phys.*, 2:91–102, 1981.

[5] V. V. Kozlov and D. V. Treshchëv. *Billiards. A Genetic Introduction to the Dynamics of Systems with Impacts*. Amer. Math. Soc., Providence, Rhode Island, 1991.

[6] A. Einstein. Zum Quantensatz von Sommerfeld und Epstein. *Verh. dt. Phys. Ges.*, 19:82–92, 1917.

[7] M. V. Berry. Regular and irregular motion. In S. Jorna, editor, *Topics in Nonlinear Dynamics*, volume No. 46 of *AIP Conference Proceedings*, pages 16–120. American Institute of Physics, New York, 1978.

[8] A. J. Lichtenberg and M. A. Lieberman. *Regular and Stochastic Motion*. Springer-Verlag, New York, 1983.

[9] R. S. MacKay. A renormalisation approach to invariant circles in area preserving maps. *Physica*, 7D:283–300, 1983.

[10] D. F. Escande. Stochasticity in classical Hamiltonian systems: Universal aspects. *Physics Reports*, 121:165–261, 1985.

[11] P. H. Richter. *Die Theorie des Kreisels in Bildern*. Report Nr. 226, Institut für Dynamische Systeme, Universität Bremen, 1990.

[12] H. R. Dullin, M. Juhnke, and P. H. Richter. The energy surfaces of the Kovalevskaya top. *Int. J. Bifurc. Chaos*, 4, 1994.

[13] L. D. Landau and E. M. Lifshitz. *Mechanics*. Pergamon Press, Oxford, New York, 1984.

[14] P. F. Byrd and M. D. Friedman. *Handbook of Elliptic Integrals for Engineers and Scientists*. Springer-Verlag, Berlin, 1971.

[15] I. S. Gradshteyn and I. M. Ryzhik. *Table of Integrals, Series, and Products*. Academic Press, New York, 1965.

[16] M. Abramowitz and I. A. Stegun. *Handbook of Mathematical Functions*. Dover Publ., New York, 1970.

[17] C. G. J. Jacobi. *Vorlesungen über Dynamik*. Chelsea Publ., New York, 1969.

[18] M. P. Kharlamov. Bifurcation of common levels of first integrals of the Kovalevskaya problem. *Prikl. Matem. Mekhan.*, 47(6):922–930, 1983.

[19] A. T. Fomenko. Topological classification of all integrable Hamiltonian differential equations of general type with two degrees of freedom. In T. Ratiu, editor, *The Geometry of Hamiltonian Systems*, volume 22 of *Math. Sci. Research Institute Publ.*, pages 131–339. Springer, New York, 1991.

[20] A. A. Oshemkov. Fomenko invariants for the main integrable cases of the rigid body motion equations. In A. T. Fomenko, editor, *Topological Classification of Integrable Systems*, volume 6 of *Advances in Soviet Mathematics*, pages 67–146. Amer. Math. Soc., Providence, Rhode Island, 1991.